ESI:

Hierarchical Cu_2S@NiCo-LDH double-shelled nanotube arrays with enhanced electrochemical performance for hybrid supercapacitors

Ze Yuan,‡[a] Haiyan Wang,‡[a] Junling Shen,[a] Pengcheng Ye,[a] Jiqiang Ning,[b] Yijun Zhong,*[a] and Yong Hu*[a]

[a]Key Laboratory of the Ministry of Education for Advanced Catalysis Materials, Department of Chemistry, Zhejiang Normal University, Jinhua 321004, China. E-mail: yonghu@zjnu.edu.cn; yonghuzjnu@163.com; yjzhong@zjnu.edu.cn

[b]Vacuum Interconnected Nanotech Workstation, Suzhou Institute of Nano-Tech and Nano-Bionics, Chinese Academy of Sciences, Suzhou 215123, China.

‡ These authors contributed equally to this work.

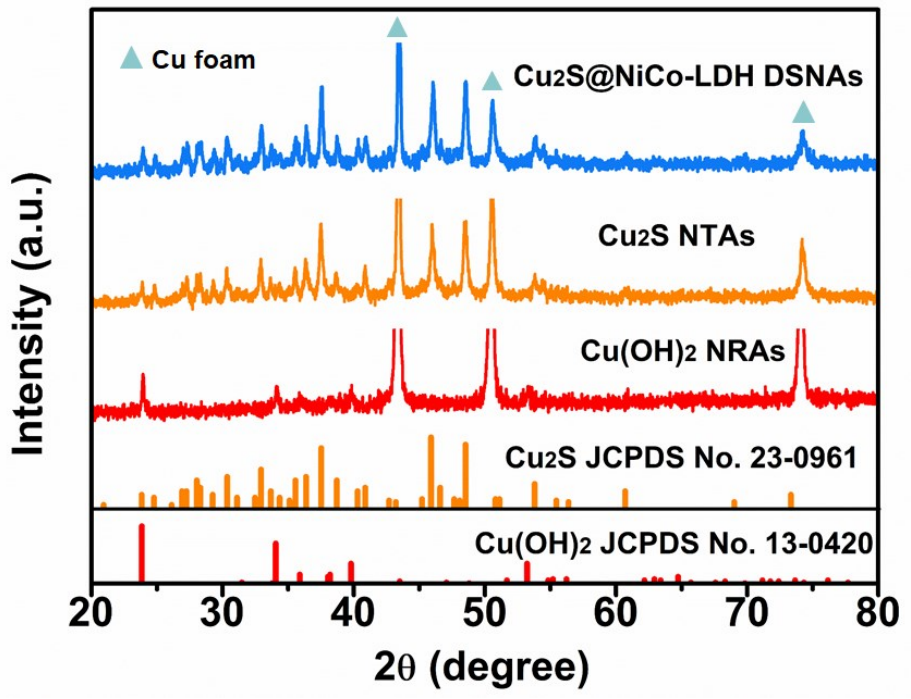

Fig. S1 XRD patterns of the as-prepared $Cu(OH)_2$ NRAs, Cu_2S NTAs and Cu_2S@NiCo-LDH DSNAs.

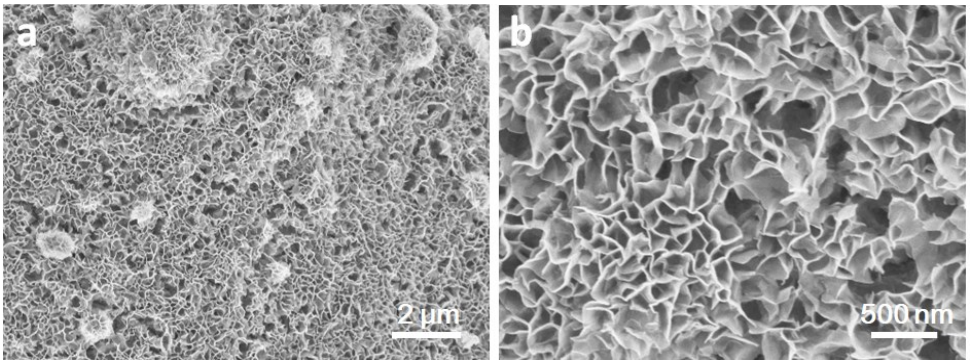

Fig. S2 FE-SEM images of the as-prepared NiCo-LDH NSs.

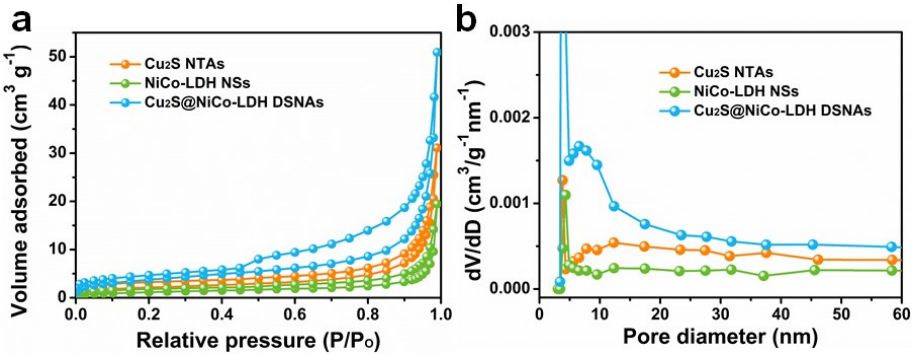

Fig. S3 (a) N_2 adsorption-desorption isotherms, and (b) pore size distribution curves of the Cu_2S@NiCo-LDH DSNAs, NiCo-LDH NSs and Cu_2S NTAs.

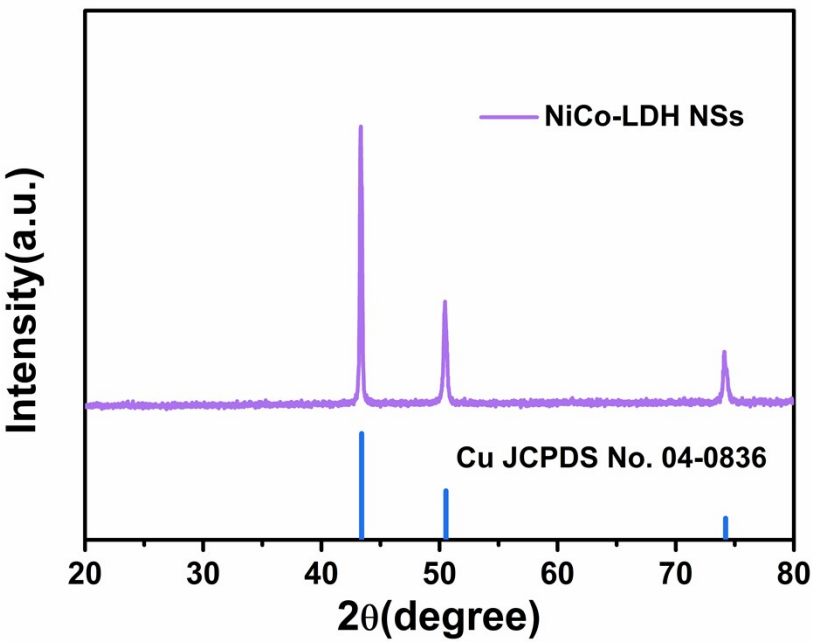

Fig. S4 XRD pattern of the as-prepared NiCo-LDH NSs.

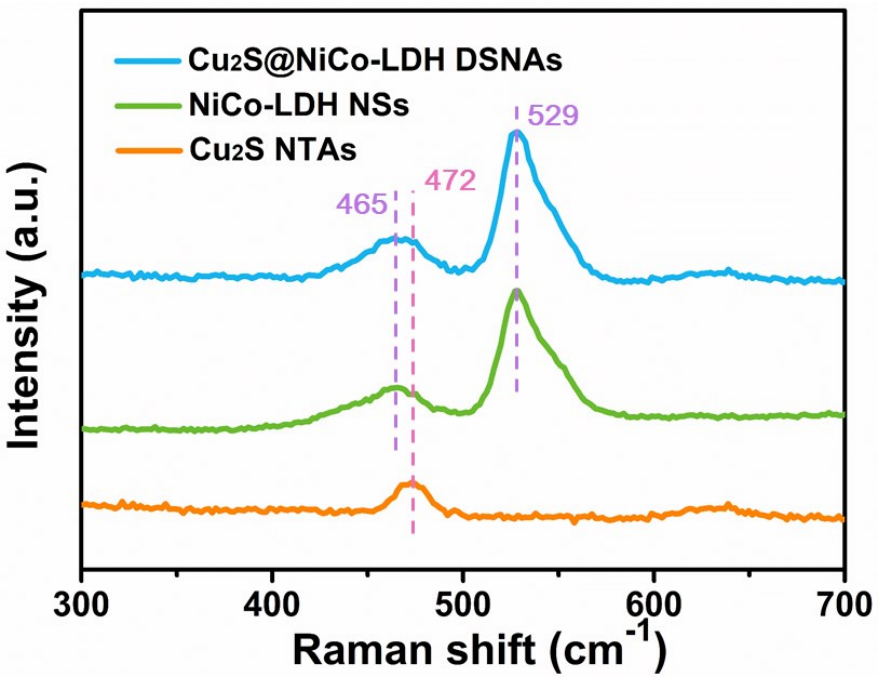

Fig. S5 Raman spectra of the Cu_2S@NiCo-LDH DSNAs, NiCo-LDH NSs and Cu_2S NTAs.

a

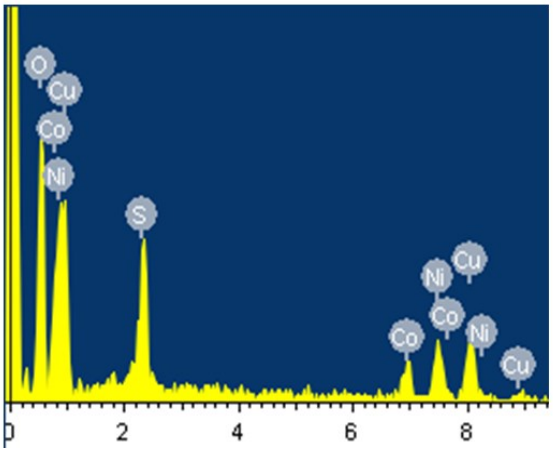

b

Element	Atomic percentage (%)
Cu	19.18
Co	6.45
Ni	14.53
O	50.41
S	9.43

Fig. S6 (a) EDX spectrum and (b) atomic percentage of the as-prepared Cu_2S@NiCo-LDH DSNAs sample.

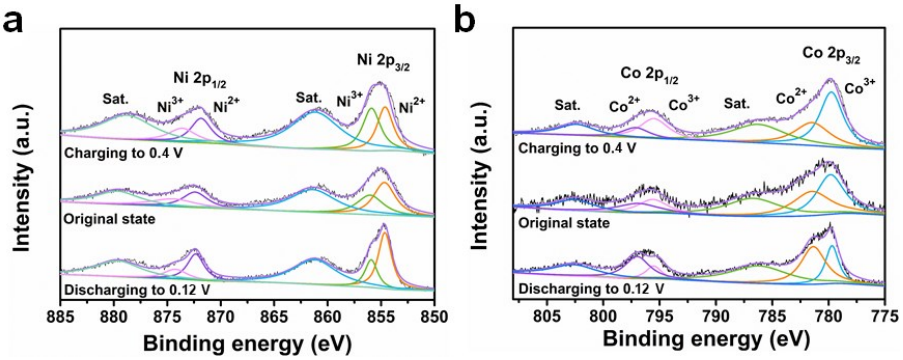

Fig. S7 The high-resolution XPS of (a) Ni 2p and (b) Co 2p of Cu_2S@NiCo-LDH DSNAs at the original state and with charge/discharge states.

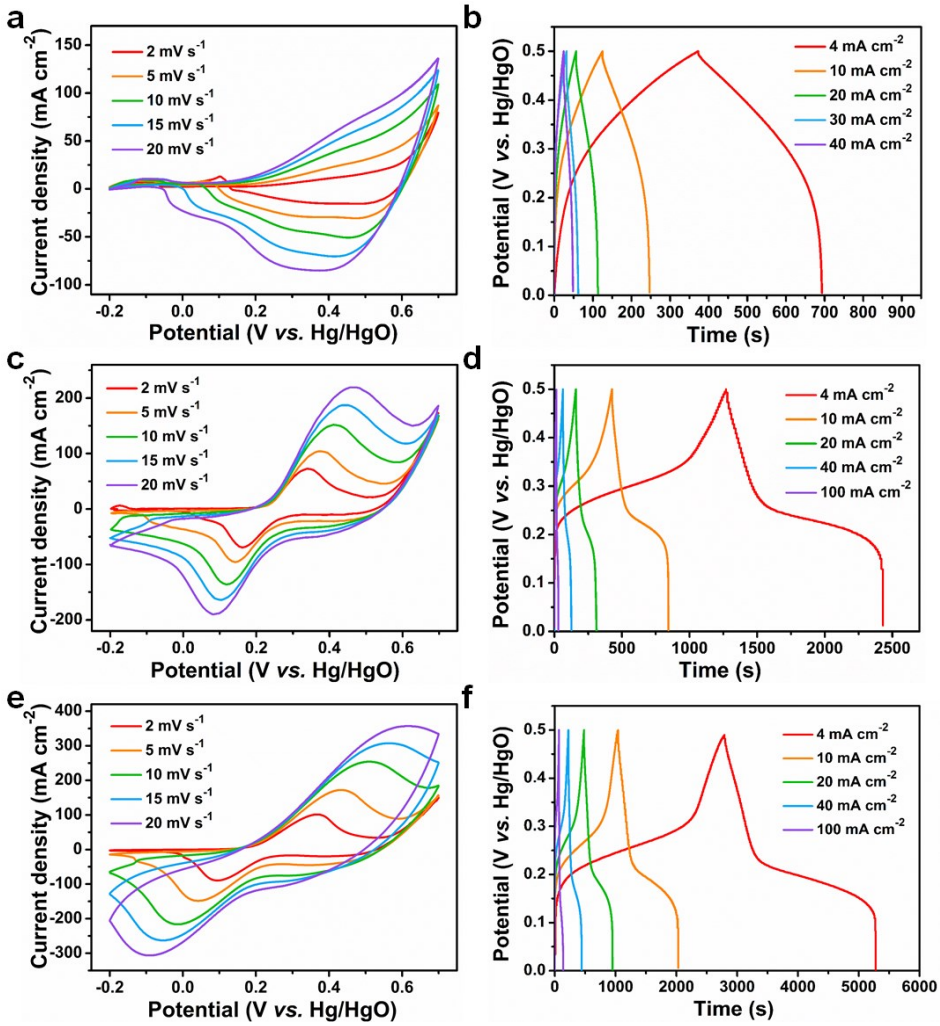

Fig. S8 CV curves of the as-prepared (a) Cu_2S NTAs, (c) NiCo-LDH NSs, (e) Cu_2S@NiCo-LDH DSNAs at various scan rates, GCD curves of (b) Cu_2S NTAs, (d) NiCo-LDH NSs, (f) Cu_2S@NiCo-LDH DSNAs at various current densities.

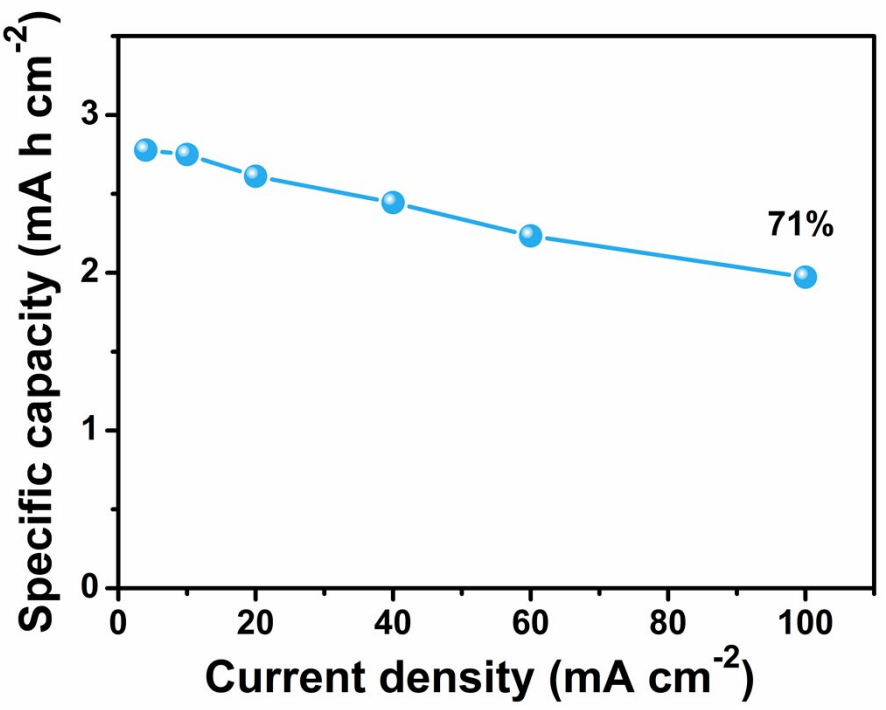

Fig. S9 The specific capacities of the Cu_2S@NiCo-LDH DSNAs at different current densities.

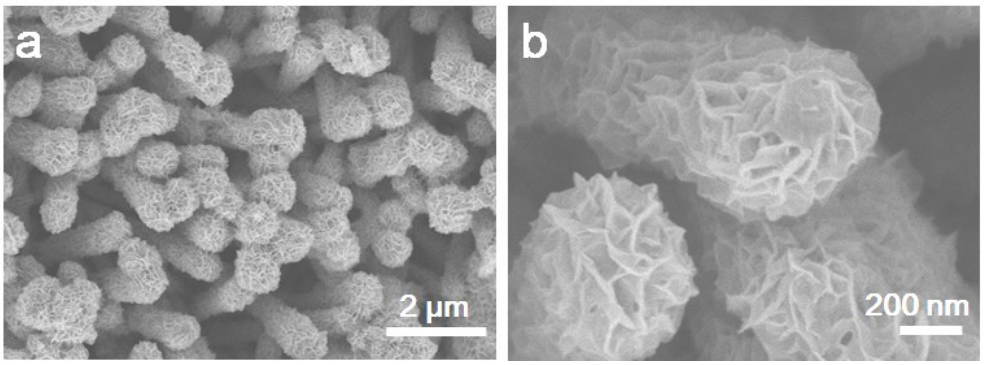

Fig. S10 (a, b) FE-SEM images of the Cu_2S@NiCo-LDH DSNAs after cyclic stability test.

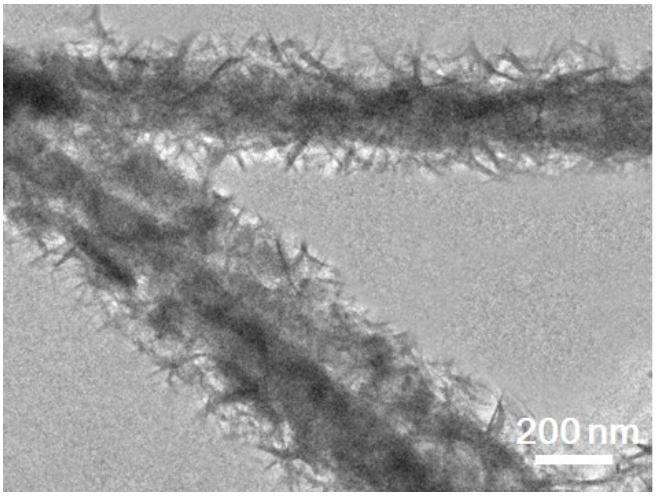

Fig. S11 TEM image of the Cu_2S@NiCo-LDH DSNAs after cyclic stability test.

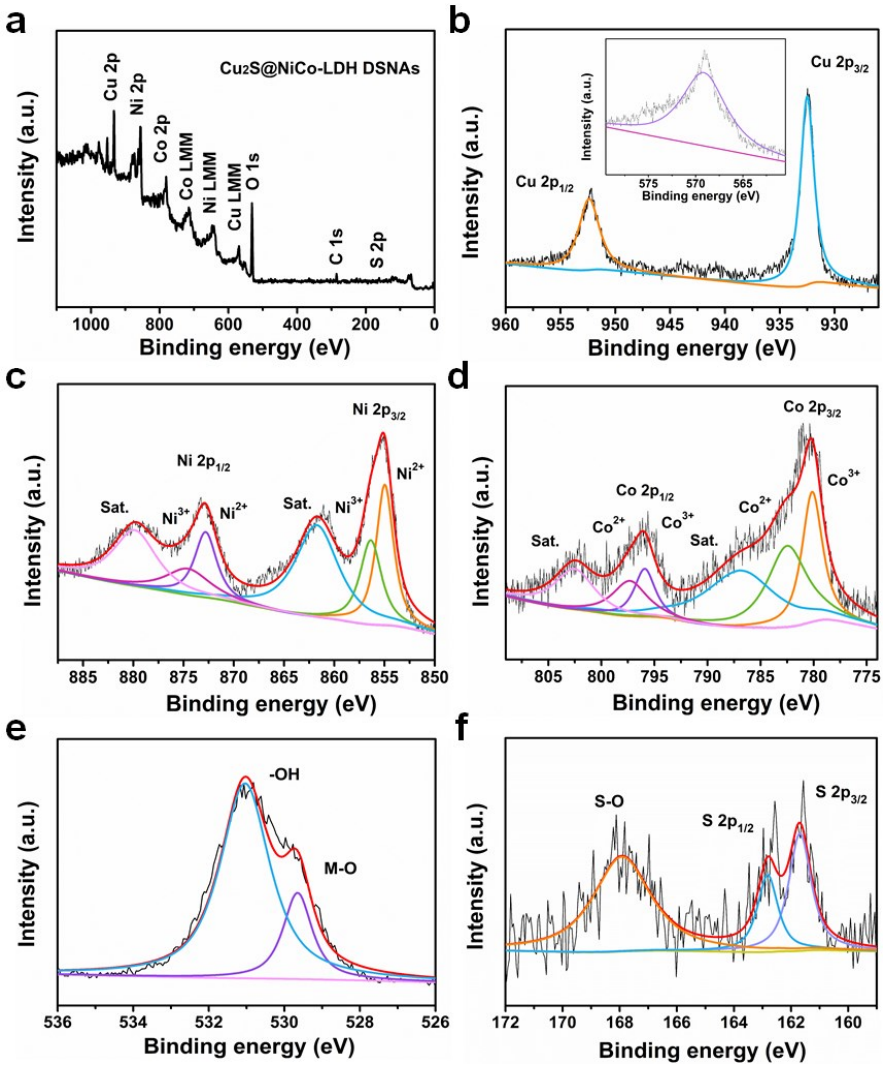

Fig. S12 XPS spectra of the Cu_2S@NiCo-LDH DSNAs after cyclic stability test. (a) Survey spectra and the high-resolution XPS of (b) Cu 2p (inset shows the Auger Cu LMM lines), (c) Ni 2p, (d) Co2p, (e) O 1s and (f) S 2p.

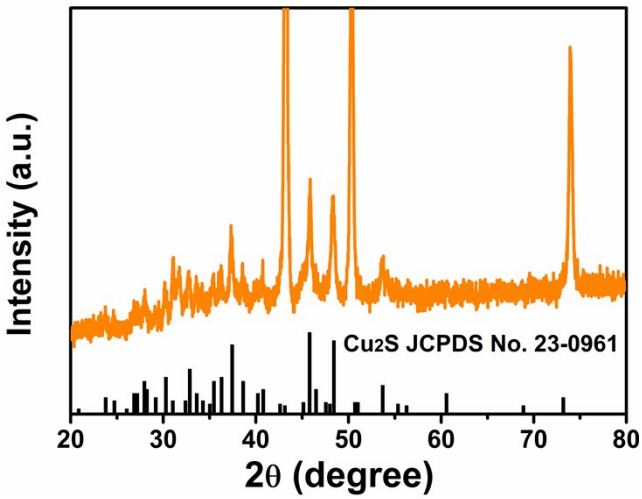

Fig. S13 XRD pattern of the Cu_2S@NiCo-LDH DSNAs after cyclic stability test.

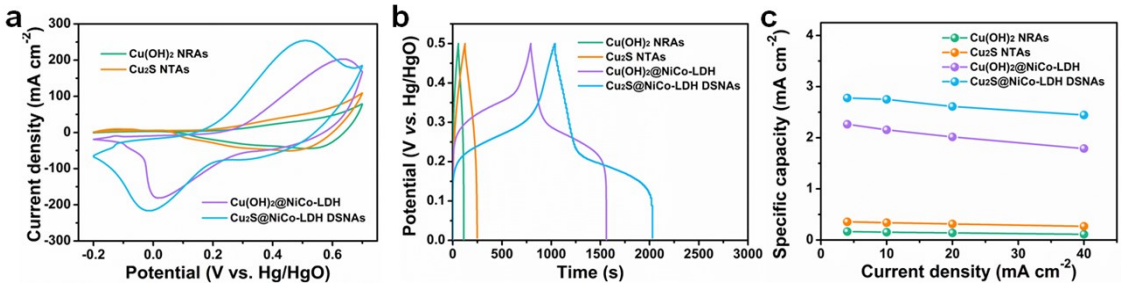

Fig. S14 Electrochemical performances of the $Cu(OH)_2$ NRAs, Cu_2S NTAs, $Cu(OH)_2$@ NiCo-LDH and Cu_2S@NiCo-LDH DSNAs. (a) CV curves at 10 mV s^{-1}. (b) GCD curves at 10 mA cm^{-2}. (c) Specific capacities at different current densities.

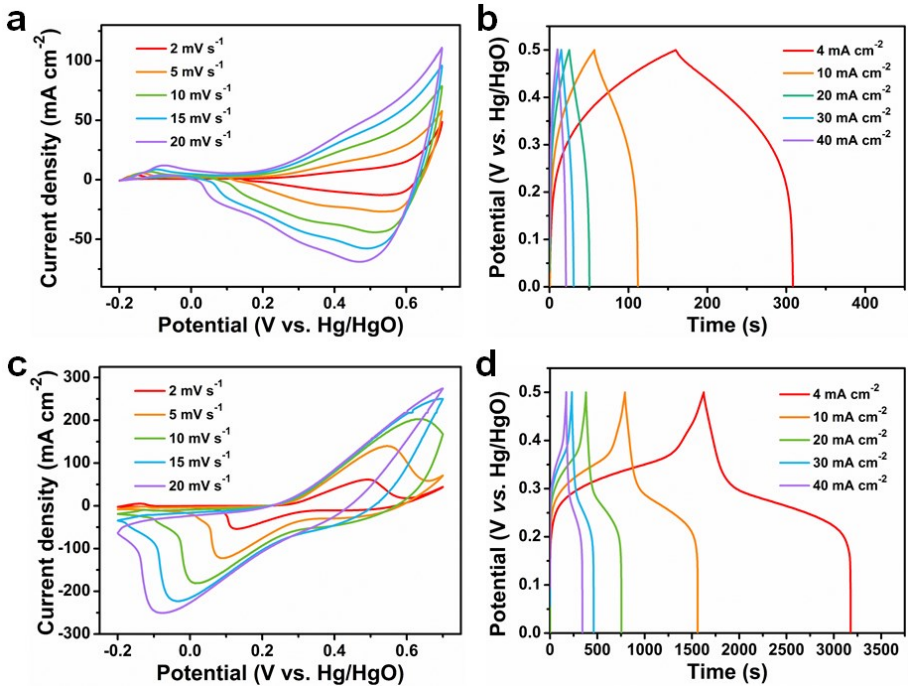

Fig. S15 CV curves of the as-prepared (a) $Cu(OH)_2$ NRAs, (c) $Cu(OH)_2$@ NiCo-LDH, at various scan rates, GCD curves of (b) Cu_2S NTAs, (d) Cu_2S@NiCo-LDH DSNAs, at various current densities.

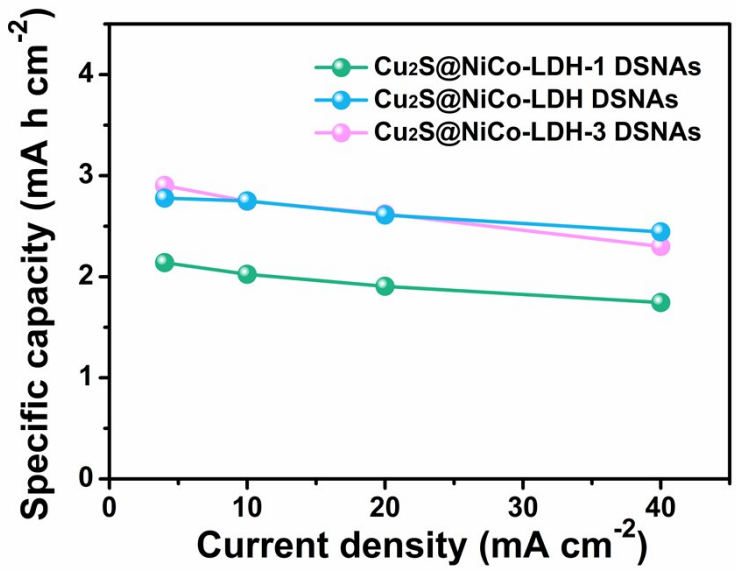

Fig. S16 Specific capacitances of Cu_2S@NiCo-LDH-1 DSNAs, Cu_2S@NiCo-LDH DSNAs and Cu_2S@NiCo-LDH-3 DSNAs at different current densities.

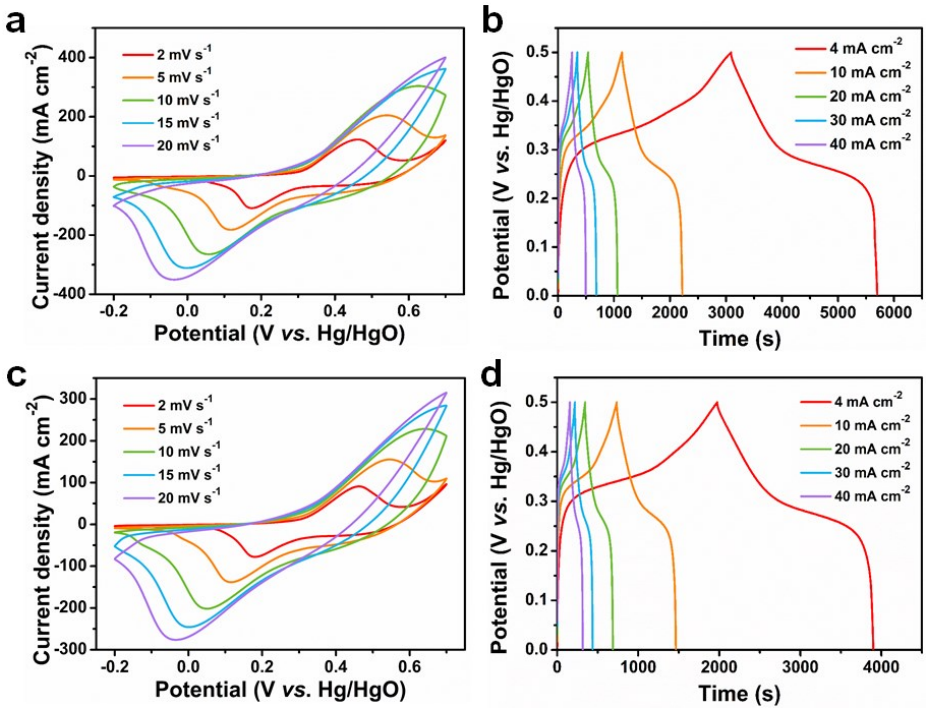

Fig. S17 (a) CV curves and (b) GCD curves of the as-prepared Cu_2S@NiCo-LDH-3 DSNAs, (c) CV curves and (d) GCD curves of the as-prepared Cu_2S@NiCo-LDH-1 DSNAs.

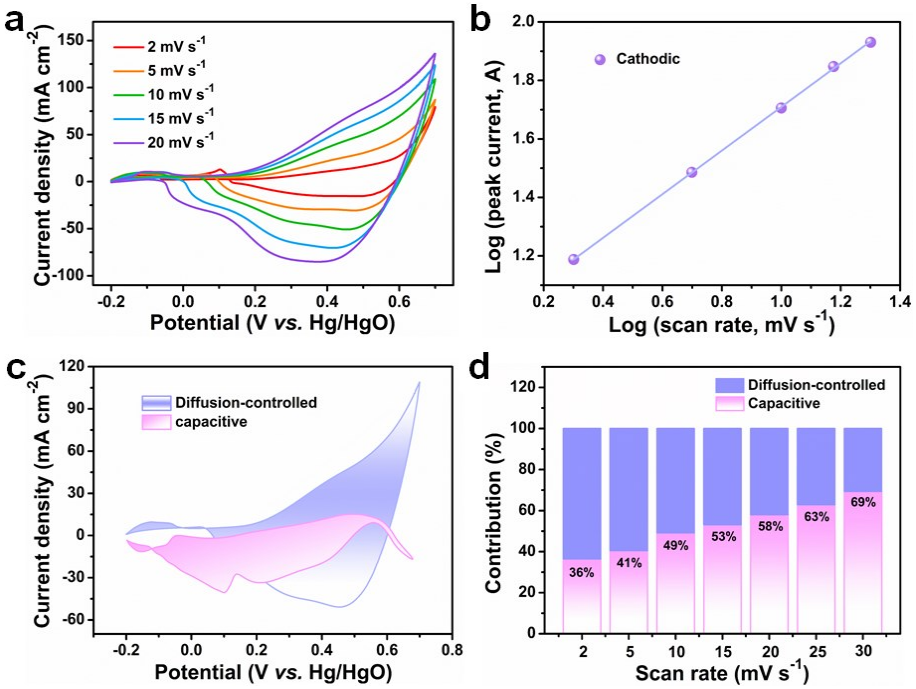

Fig. S18 (a) The CV curves of the Cu_2S NTAs electrode at different scan rates. (b) The plot of log(i) versus log(v). (c) Separation of the diffusion and capacitive-controlled currents of the Cu_2S NTAs electrode at a scan rate of 10 mV s^{-1}. (d) Relative contribution of the diffusion and capacitive-controlled charge storage at different scan rates.

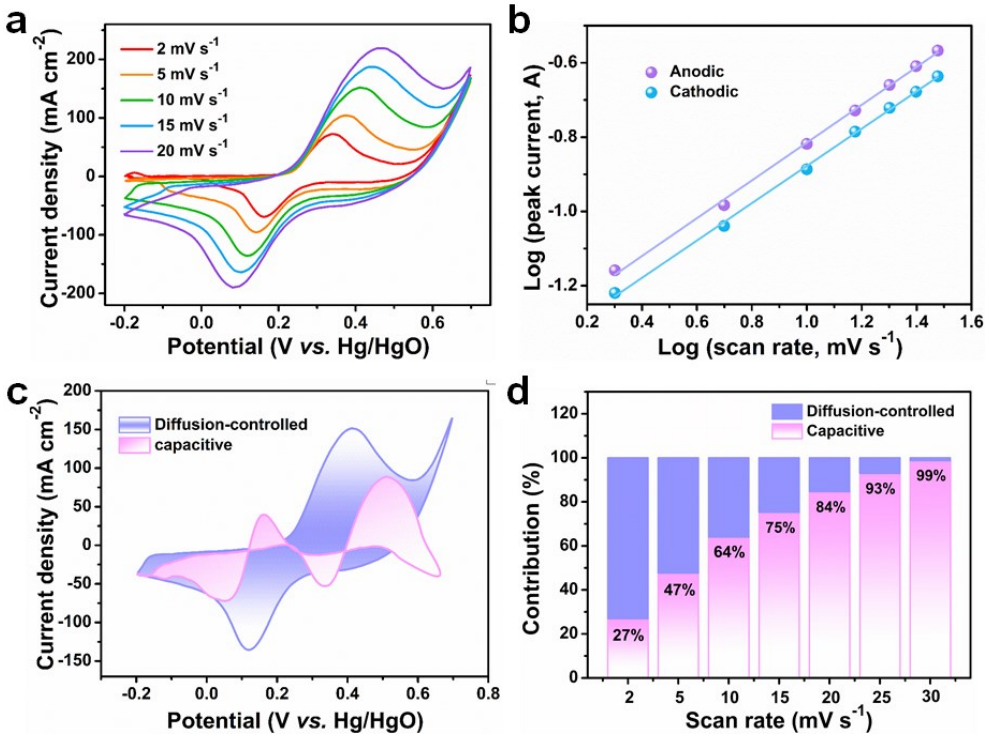

Fig. S19 (a) The CV curves of the NiCo-LDH NSs electrode at different scan rates. (b) The plot of log(i) versus log(v). (c) Separation of the diffusion and capacitive-controlled currents of the NiCo-LDH NSs electrode at a scan rate of 10 mV s^{-1}. (d) Relative contribution of the diffusion and capacitive-controlled charge storage at different scan rates.

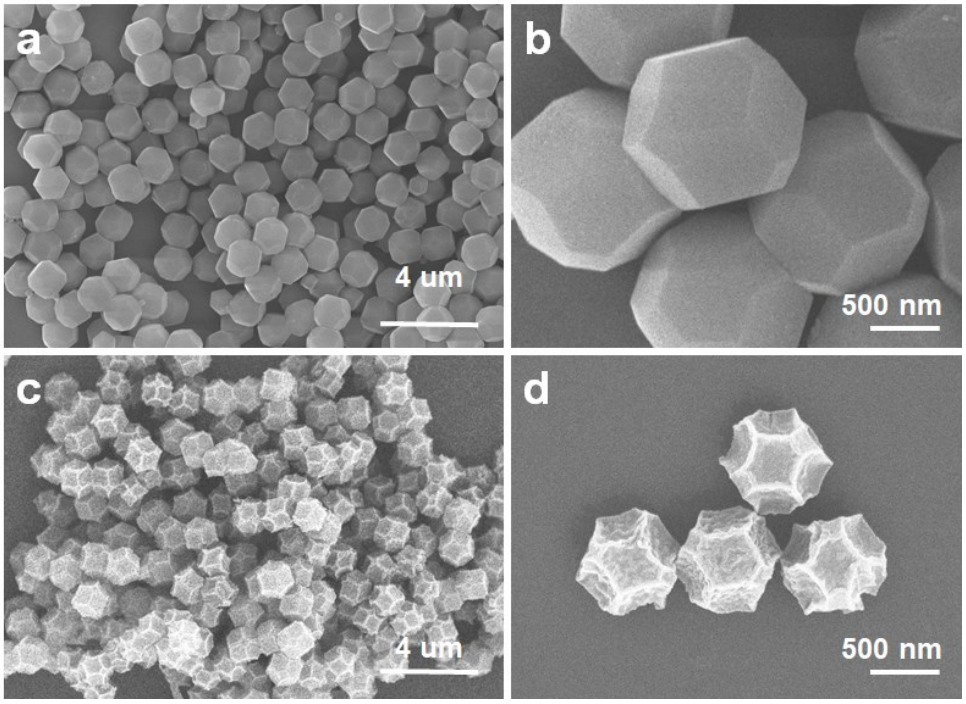

Fig. S20 The FE-SEM images of the as-prepared (a, b) ZIF-8 and (c, d) NPC.

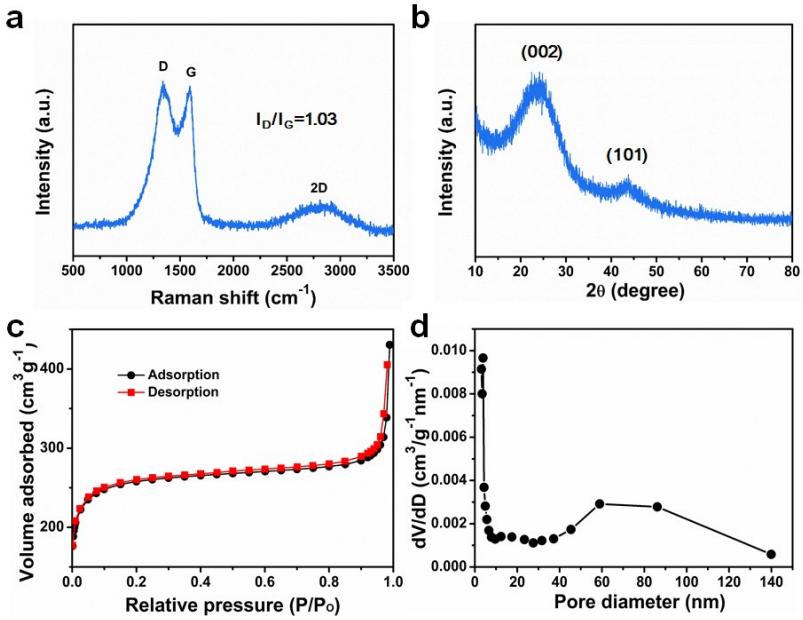

Fig. S21 Structural characterization of the as-prepared NPC: (a) Raman; (b) XRD pattern; (c) N_2 adsorption isotherms and (d) pore size distribution.

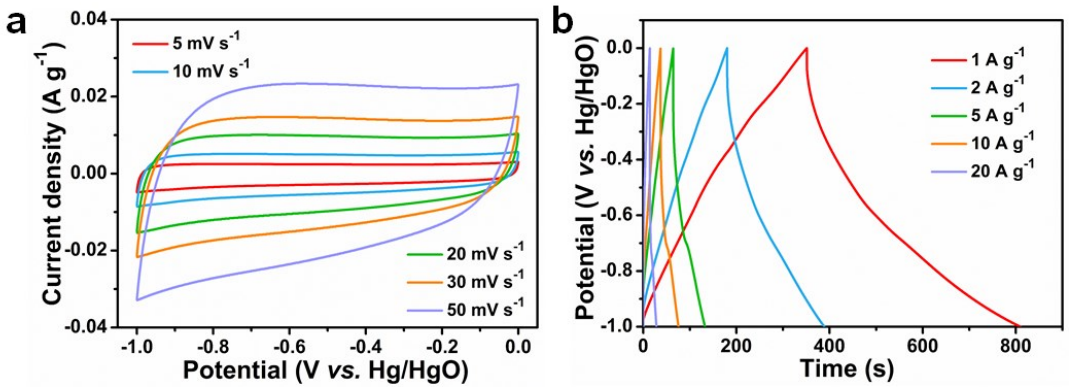

Fig. S22 (a) CV curves and (b) GCD curves of the as-prepared NPC.

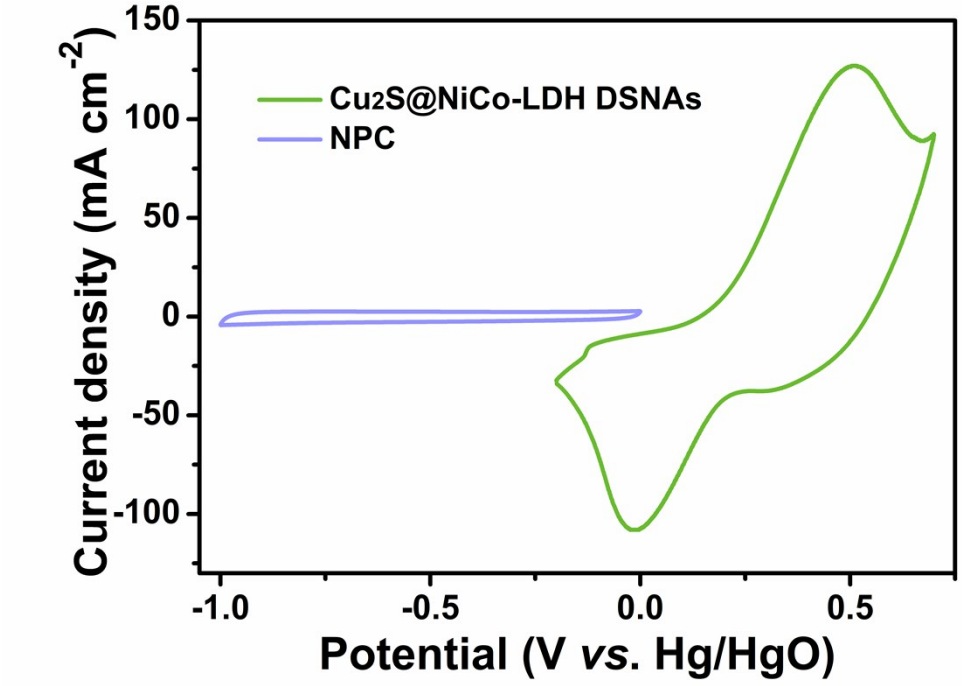

Fig. S23 CV curves of the Cu_2S@NiCo-LDH DSNAs and NPC at 10 mV s^{-1}.

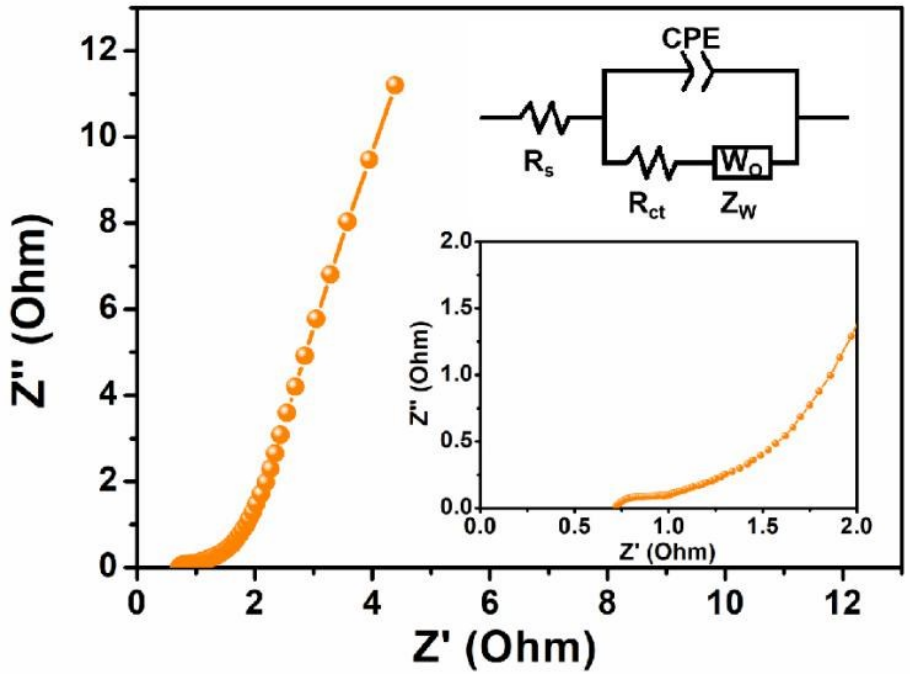

Fig. S24 EIS spectrum of the Cu_2S@NiCo-LDH DSNAs//NPC HSC device with the insets of the EIS spectrum in high-frequency region and the simulated circuit diagram, respectively.

Table S1 Comparative areal capacity values (measured in three-electrode system) of the previously reported transition metal hydroxides-based electrodes with our Cu_2S@NiCo-LDH DSNAs.

Electrode material	Electrolyte	Current density (mA cm^{-2})	C_a (F cm^{-2})	Ref.
Cu_2S@NiCo-LDH DSNAs	**6 M KOH**	**4**	**20.40**	**This work**
Cu_3N@CoFe-LDH	2 M KOH	1	3.08	S1
$Co(OH)_2$/HNNF	2 M KOH	5	3.17	S2
Zn–Ni–Co TOH	1 M KOH	3	2.14	S3
CuO@CoFe-LDH NWAs	1 M KOH	2.5	0.87	S4
NC LDH NFAs@NSs/Ni	1 M KOH	2	1.46	S5
$ZnCo_2O_4$@$Ni_xCo_{2x}(OH)_{6x}$	2 M KOH	5	3.35	S6
$CoNiO_2$ NWAs@$Ni(OH)_2$ NSs/CNTF	3 M KOH	1	6.06	S7

Table S2 Fitting results of the EIS data

Sample	R_s (Ω)	R_{ct} (Ω)	CPE-P (mF)	CPE-T (mF)	W-R (Ω)	W-T (Ω)	W-P (Ω)
Cu_2S NTAs	**0.80**	**0.02**	**0.66**	**1.05**	**0.60**	**0.80**	**0.49**
NiCo-LDH NSs	**0.64**	**0.05**	**0.67**	**0.31**	**1.96**	**2.79**	**0.38**
Cu_2S@NiCo-LDH DSNAs	**0.61**	**0.01**	**1.18**	**0.01**	**0.48**	**1.30**	**0.40**

Table S3 Comparative areal capacitances, areal energy and power densities of recently reported HSCs with our HSCs.

Electrode material	C_a (F cm^{-2})	E_a (mW h cm^{-2})	P_a (mW cm^{-2})	Ref.
Cu_2S@NiCo-LDH DSNAs	**4.2**	**1.67**	**4.25**	**This work**
$CoMoO_4$@$Co(OH)_2$/CT//PAC	0.5	0.17	1.50	S8
NC LDH NSs@Ag@CC//AC	0.2	0.08	0.80	S9
$NiCo_2O_4$@$Co_{0.33}Ni_{0.67}(OH)_2$//CMK-3-ASC	0.9	0.32	4.00	S10
ZNCO@$Ni(OH)_2$//VN@C	0.6	0.20	2.40	S11
NC LDH NFAs@NSs/Ni//AC@CF	1.2	0.40	2.40	S5
$Ni(OH)_2$–Cu//RGO	2.5	0.95	2.01	S12
$NiCo_2S_4$//C	0.5	0.12	0.80	S13
Cu_3N@CoFe-LDH//AC	1.2	0.42	1.70	S1

Reference

1. X. Zhou, X. Li, D. Chen, D. Zhao and X. Huang, *J. Mater. Chem. A*, 2018, **6**, 24603-24613.
2. Z. Yu, Z. Cheng, X. Wang, S. X. Dou and X. Kong, *J. Mater. Chem. A*, 2017, **5**, 7968-7978.
3. Z. Huang, F. Sun, M. Batmunkh, W. Li, H. Li, Y. Sun, Q. Zhao, X. Liu and T. Ma, *J. Mater. Chem. A*, 2019, **7**, 11826-11835.
4. Z. Li, M. Shao, L. Zhou, R. Zhang, C. Zhang, J. Han, M. Wei, D. Evans and X. Duan, *Nano Energy*, 2016, **20**, 294-304.
5. G. Nagaraju, S. Sekhar, L. Bharat and J. Yu, *ACS Nano*, 2017, **11**, 10860-10874.
6. W. Fu, Y. Wang, W. Han, Z. Zhang, H. Zha and E. Xie, *J. Mater. Chem. A*, 2016, **4**, 173-182.
7. Q. Li, Q. Zhang, J. Sun, C. Liu, J. Guo, B. He, Z. Zhou, P. Man, C. Li, L. Xie and Y. Yao, *Adv. Sci.*, 2019, **6**, 1801379.
8. G. Veerasubramani, A. Chandrasekhar, S. M. S. P, Y. Mok and S. Kim, *J. Mater. Chem. A*, 2017, **5**, 11100-11113.
9. S. Sekhar, G. Nagaraju and J. Yu, *Nano Energy*, 2017, **36**, 58-67.
10. K. Xu, R. Zou, W. Li, Q. Liu, X. Liu, L. An and J. Hu, *J. Mater. Chem. A*, 2014, **2**, 10090-10097.
11. Q. Zhang, W. Xu, J. Sun, Z. Pan, J. Zhao, X. Wang, J. Zhang, P. Man, J. Guo, Z. Zhou, B. He, Z. Zhang, Q. Li, Y. Zhang, L. Xu and Y. Yao, *Nano Lett.*, 2017, **17**, 7552-7560.
12. D. Shi, L. Zhang, X. Yin, T. J. Huang and H. Gong, *J. Mater. Chem. A*, 2016, **4**, 12144-12151.
13. W. Kong, C. Lu, W. Zhang, J. Pu and Z. Wang, *J. Mater. Chem. A*, 2015, **3**, 12452-12460.